

# The influence of interaction between oxygen vacancies on set process in resistive switching: A case of MgO

Cite as: AIP Advances **9**, 055230 (2019); <https://doi.org/10.1063/1.5092690>

Submitted: 13 February 2019 • Accepted: 22 May 2019 • Published Online: 31 May 2019

Yanrui Guo, Qinggong Song and Huiyu Yan



[View Online](#)



[Export Citation](#)



[CrossMark](#)

## ARTICLES YOU MAY BE INTERESTED IN

**Band gap and defect states of MgO thin films investigated using reflection electron energy loss spectroscopy**

AIP Advances **5**, 077167 (2015); <https://doi.org/10.1063/1.4927547>

**Conduction mechanism of resistive switching films in MgO memory devices**

Journal of Applied Physics **111**, 094104 (2012); <https://doi.org/10.1063/1.4712628>

**Engineering of defects in resistive random access memory devices**

Journal of Applied Physics **127**, 051101 (2020); <https://doi.org/10.1063/1.5136264>

Call For Papers!

**AIP Advances**

**SPECIAL TOPIC: Advances in Low Dimensional and 2D Materials**

# The influence of interaction between oxygen vacancies on set process in resistive switching: A case of MgO

Cite as: AIP Advances 9, 055230 (2019); doi: 10.1063/1.5092690

Submitted: 13 February 2019 • Accepted: 22 May 2019 •

Published Online: 31 May 2019



View Online



Export Citation



CrossMark

Yanrui Guo, Qinggong Song, and Huiyu Yan<sup>a)</sup>

## AFFILIATIONS

College of Science, Civil Aviation University of China, Tianjin 300300, China

<sup>a)</sup>Corresponding author. Tel./fax.: +86 22 24092514 E-mail address: huiyu\_yan@163.com

## ABSTRACT

The influence factor of filaments consisted of oxygen vacancies ( $V_{Os}$ ) is important for resistive switching. In this paper, the interaction between  $V_{Os}$  in MgO and its influence on  $V_O$ -filaments are studied using density functional theory. It reveals that the  $V_{Os}$  in MgO tend to be aggregation state. The distribution of energy level for  $V_O$  pair in band gap changes with different configurations. The interaction between  $V_O$  chains also results in their aggregation state in MgO insulator. The calculation results show that with the diameter of filament increasing, the formation energy per  $V_O$  decreases and the filaments presents semiconductor-metal transition. Based on these calculation results, the set process of MgO based resistive switching is discussed.

© 2019 Author(s). All article content, except where otherwise noted, is licensed under a Creative Commons Attribution (CC BY) license (<http://creativecommons.org/licenses/by/4.0/>). <https://doi.org/10.1063/1.5092690>

## INTRODUCTION

Resistive switching (RS) effect has attracted much attention of researchers because its application in resistance random access memory (RRAM) and neuromorphic computing.<sup>1–3</sup> The resistive switching effect can be realized in most of oxides, such as NiO, TaO<sub>x</sub>, HfO<sub>2</sub>, MgO, et al.<sup>4–13</sup> The mechanism of RS of oxides is still an open topic till now. A widely accepted explanation of RS is the growth and rupture of conductive filament.<sup>7–11</sup> According to this model, the filaments consisted of oxygen vacancies ( $V_{Os}$ ) grow from bottom electrode to top electrode during set process, and can be ruptured by reverse bias or joule heat during reset process. However, the process of  $V_O$ -filament growth is unknown yet, which is important for properties of filaments and thus RS types.<sup>14</sup> According to the reported results, there are many factors contributing to properties of filaments, such as set voltage; compliance current; the structure of insulator et al. In this paper, using first-principles method, we draw our aims on the influence of interaction between  $V_{Os}$  on formation of  $V_O$ -filament in MgO based RSs. MgO film is a less studied material but has great potential application in RRAMs.<sup>12,13,15</sup> Huang et al. have found that Pt/MgO/Pt devices show nonpolar RS.<sup>16</sup> Dias reported the coexistence of unipolar and bipolar RS in

Pt/MgO/Ta system.<sup>17</sup> The formation and rupture of  $V_O$ -filaments in MgO are suggested to response for MgO based RS in these literatures.<sup>15–17</sup> However, the formation mechanism of  $V_O$ -filaments and its influence on the change in resistance of device are still unclear. Therefore, the interaction of  $V_{Os}$  and its influence on formation of  $V_O$ -filaments is discussed in this paper. It is important not only for understanding the MgO based RS, but also for understanding the mechanism of RS behaviors metal oxide.

## EXPERIMENT METHOD

The first-principles calculations are performed by the CASTEP package in Materials Studio (MS) software.<sup>18</sup> The interaction between the electrons and the ionic cores are described by ultra-soft pseudopotential.<sup>19</sup> The exchange correlation interactions are described by generalized gradient approximation (GGA) within Perdew–Burke–Ernzerhof (PBE) scheme.<sup>20</sup> The geometrical structure optimizations in our calculations are performed by using the Broyden–Fletcher–Goldfarb–Shanno (BFGS) formula.<sup>21</sup> The electrons  $2p^63s^2$  for Mg and  $2s^22p^4$  for O are considered as the valence states. The kinetic energy cutoff of plane wave was 420 eV and the SCF tolerance was  $5 \times 10^{-7}$  eV/atom. The maximum

displacement, the force per atom and the maximum stress are lower than  $5 \times 10^{-4}$  Å, 0.01 eV/Å and 0.02 GPa, respectively.

## RESULTS AND DISCUSSION

Pure MgO presents rocksalt cubic structure with parameters  $a=4.21$  Å. After a full geometrical structure relaxation without any restriction, we get the calculated lattice parameters of MgO,  $a=4.296$  Å, which is good agreement with experimental and other calculated results.<sup>22,23</sup> This means the methods of our calculation is reasonable. The calculated band gap of pure MgO is 4.24 eV, which is in accord with other reported calculated results, but smaller than experiment results.<sup>23,24</sup> This comes from the underestimated of band gap by density functional theory (DFT). To research the formation energy of  $V_O$  defects and the interaction between  $V_O$ s, we build a  $2 \times 2 \times 2$  supercell of MgO based on tradition MgO cell, as shown in Figure 1. We delete one oxygen atom in the supercell to get the model of  $V_O$  defects in MgO. For  $2 \times 2 \times 2$  supercell based systems, a  $3 \times 3 \times 3$  K-point mesh was selected in all Brillouin zones after  $K$  points test with Monkhorst-Pack method.<sup>25</sup> After geometry optimization, we can get energy of in MgO with  $V_O$  defect. The formation energy of  $V_O$  defect can be calculated by formula:<sup>26</sup>

$$E_{form} = E_{defect} - E_{MgO} + n\mu_O$$

Where  $E_{defect}$  is the total energy of MgO supercell containing oxygen vacancies;  $E_{MgO}$  is the total energy of equivalent perfect supercell;  $n$  is the number of oxygen atoms removed from the perfect MgO supercell and  $\mu_O$  is the corresponding chemical potential of oxygen. Oxygen potential is determined by conditions of the phases containing magnesium and oxygen atoms. Under the Mg rich condition,  $\mu_O$  could be defined as

$$\mu_O = E_{MgO} - \mu_Mg$$

where  $E_{MgO}$  is the energy of a primary cell of MgO;  $\mu_Mg$  is the chemical potential of an Mg atom, which equals energy of one Mg atom in bulk Mg. Under the oxygen rich condition,  $\mu_O$  equals energy of

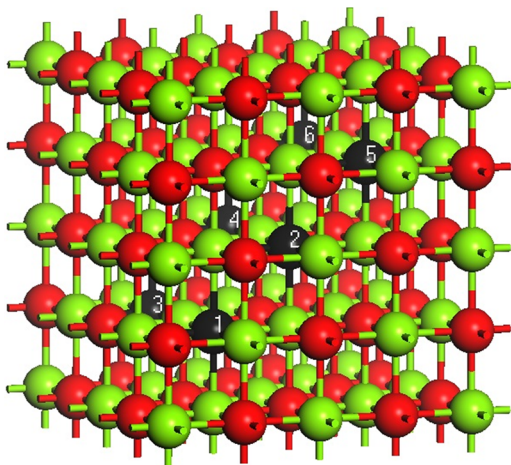


**FIG. 1.** A  $2 \times 2 \times 2$  supercell of MgO for calculation, in which the red and the green balls denote the oxygen and magnesium atoms, respectively. The black balls denote oxygen atoms which will be deleted in  $V_O$ -pairs calculations.

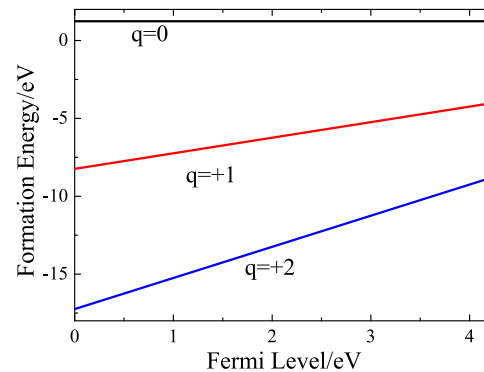
one oxygen atom in  $O_2$  molecule, which comes from the calculation results of an isolated  $O_2$  molecule within a cubic box of  $10 \times 10 \times 10$  Å<sup>3</sup>. During the calculation of the chemical potential of the oxygen atom, the triplet state of  $O_2$  is employed and only the  $G$  point was used. The formation energy is 1.24 eV and 6.65 eV for Mg rich and O rich conditions, respectively. Therefore, the  $V_O$  defects are easier to form under Mg-rich condition than under O-rich condition. This can give a clue to understand the clustering characters of  $V_O$  defects discussed in the next text.

Considering the defect in MgO can take vary charge state,<sup>27</sup> we have calculate the formation energy of charged oxygen vacancy by formula:

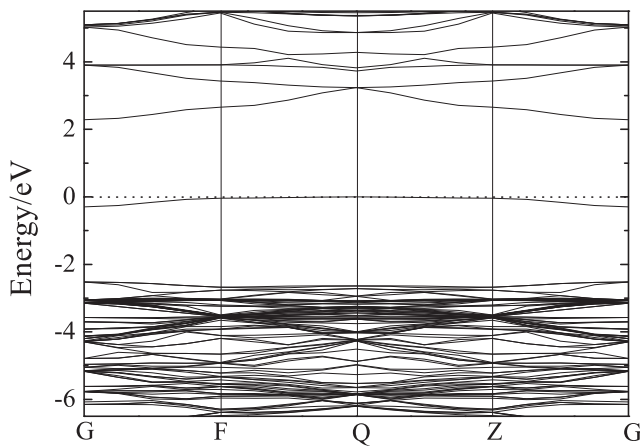
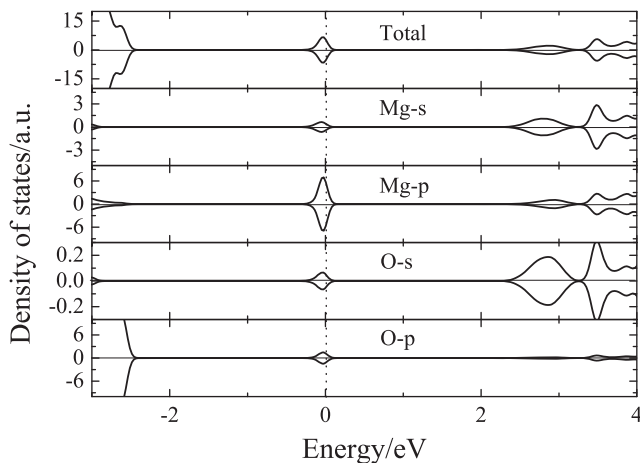
$$E_{form}^q = E_{defect}^q - E_{MgO} + n\mu_O + qE_F$$

In which  $q$  is the charge state of system and  $E_F$  is the Fermi level. The formation energy of  $V_O$  with various charge states as a function of Fermi level is shown in figure 2, from which we can find that  $V_O$ s prefer 2+ charge states. The formation energies in our calculations are lower than the values reported in some literatures.<sup>28,29</sup> This may comes from the difference in calculation method. Meanwhile, the large formation energy always means more difficulty in fabrication experimentally. The moderate formation energy of  $V_O$  under Mg rich condition in our calculation indicates  $V_O$  defects can be formed under certain experiment conditions. As a matter of fact, in MgO based RS cell, many  $V_O$  defects exist in MgO insulator during RS process.<sup>12,13</sup> It should be noted that, as reported, with the different fabrication process, both Mg-rich and Mg-deficient films all can be realized in experiments.<sup>12,16</sup> On the other hand, formation energy is not the only influence element for RS effect. As reported, in Mg-deficient films, oxygen atom at interstitial lattice is beneficial for migration of oxygen ions and thus for RS effect.<sup>12</sup> As a result, RS effect and the  $V_O$  filaments can be realized in both Mg-rich and Mg-deficient MgO films.

The calculated band structure of MgO supercell with one  $V_O$  defect is shown in Figure 3. It can be see that the impurity level locates at the 2.3 eV below bottom of conduction band. Considering the underestimate of DFT on bandgap, the gap between impurity level and bottom of conduction band should be larger than our result. Figure 4 is the corresponding total and partial density of states (DOS). We can find the impurity band mainly comes from Mg-2p electrons while valance band are mainly contributed by O-2p states.



**FIG. 2.** The formation energy of  $V_O$  as a function of Fermi level.

FIG. 3. The band structure of MgO supercell with one  $V_O$  defect.FIG. 4. The total and partial density of states for MgO supercell with one  $V_O$  defect.

To explore the possible structures of  $V_O$ -filament in MgO, we have investigated the interaction between two  $V_O$ s with variable configurations. As shown in figure 1, in a  $2\times 2\times 2$  supercell of MgO, we delete two  $V_O$ s with different configurations to construct  $V_O$  pair models. There are five different configurations of  $V_O$  pair, (1, 2), (1, 3), (1, 4), (1, 5) and (1, 6). The formation energy per  $V_O$  defect for various configuration is shown in Table I. It shows that the (1, 2) configuration, in which the two  $V_O$ s are nearest neighbor, takes the least energy. This means the  $V_O$  defects in MgO present aggregation effect. On the other hand, one can find that the formation energy

TABLE I. Formation energy per oxygen vacancy for isolated and  $V_O$  pair with different configuration.

configuration	isolated	(1, 2)	(1, 3)	(1, 4)	(1, 5)	(1, 6)
Formation Energy (eV)	1.241	1.207	1.262	1.257	1.253	1.251

for other configurations  $V_O$  pair is larger than that for isolated  $V_O$  slightly, which might come from the distortion of lattice.

Figure 5 and Figure 6 show band structures and corresponding total density of states for different  $V_O$  pairs, from which we can find there are much difference among them. The electron structure of configuration (1, 6) is similar to isolated  $V_O$ , which can be considered as a result of large distance between two  $V_O$ s in configuration (1, 6). For configurations (1, 2-5), it is interesting to find that two impurity bands in band gap separate with the decreasing of formation energy. It suggests that the interaction between  $V_O$ s can decrease the system energy. As two  $V_O$ s are introduced in the supercell, the corresponding lattice distortions and excess electrons will start to interact. At the same time the polaronic effects arise, which can redistribute the excess electrons to minimize the coulomb repulsion. Since the  $V_O$  pair with nearest distance shows the least formation energy, it can be conclude that the  $V_O$  chain growth mainly along [110] crystal orientation during set process in RS.

To construct one continued  $V_O$ -chain in MgO, based on an MgO primary cell, we build a  $4\times 4\times 3$  supercell (96 atoms) and delete three oxygen atoms along [110] crystal orientation, as shown in Figure 6a. After geometrical structure relaxation and energy calculation, we can get the electronic properties of system. As shown in Table II the formation energy per  $V_O$  in this model is 1.133 eV, which is smaller than isolated  $V_O$  in MgO supercell significantly. This can be regarded as a result of interaction between  $V_O$ s. In addition, we have tested the cohesive energy of one  $V_O$ -chain. Four oxygen atoms are deleted from a  $2\times 2\times 2$  supercell (64 atoms) of MgO along [110] crystal orientation, forming a  $V_O$ -chain model. The cohesive energy of  $V_O$  chain with different charge states are calculated using the formula:

$$E_c(q) = E(V_O^q - \text{chain}) + 3 \times E(\text{bulk}) - 4 \times E(\text{isolated} - V_O^q) \quad (1)$$

Where  $E(V_O^q - \text{chain})$  is the energy of supercell containing  $V_O$  chain,  $E(\text{bulk})$  is the energy of  $2\times 2\times 2$  supercell (64 atoms) of MgO, and  $E(\text{isolated} - V_O^q)$  is the energy is the energy of supercell containing one  $V_O$  defect. Our calculation results indicate the  $V_O$  chain with 2+ charge state possess the lowest cohesive energy. Therefore,  $V_O$  chain is easier to form with 2+ charge state compared with 1+ and 0 charge states.

To test the lowest energy configuration, the calculation for energy of  $V_O$  clusters is performed. In a  $4\times 4\times 3$  supercell (64 atoms), six nearest neighbor oxygen atoms are deleted to simulate the oxygen cluster. The formation energy per  $V_O$  for cluster configuration is 1.05 eV, which is smaller than one  $V_O$ -chain model slightly. However, during set process in resistance switching, the  $V_O$  defect tend to formed in chains configuration because of the breakdown field although the cluster configuration takes lowest formation energy.

To study the influence of the interaction between  $V_O$ -chains on characters of  $V_O$ -filaments, as shown in figure 7b and 7c, based on a 96 atoms supercell, we build double  $V_O$ -chain models with different states, nearest neighbor state and separation state, respectively. After geometry optimization, we can get the different energy between two states. For double  $V_O$ -chains, the energy of separation state is 0.15 eV per  $V_O$  higher than that of nearest neighbor state. Therefore, the interaction between two  $V_O$ -chains can result in the lower energy of system. This means the  $V_O$ -filaments tend to be aggregation state during the set process in RS.

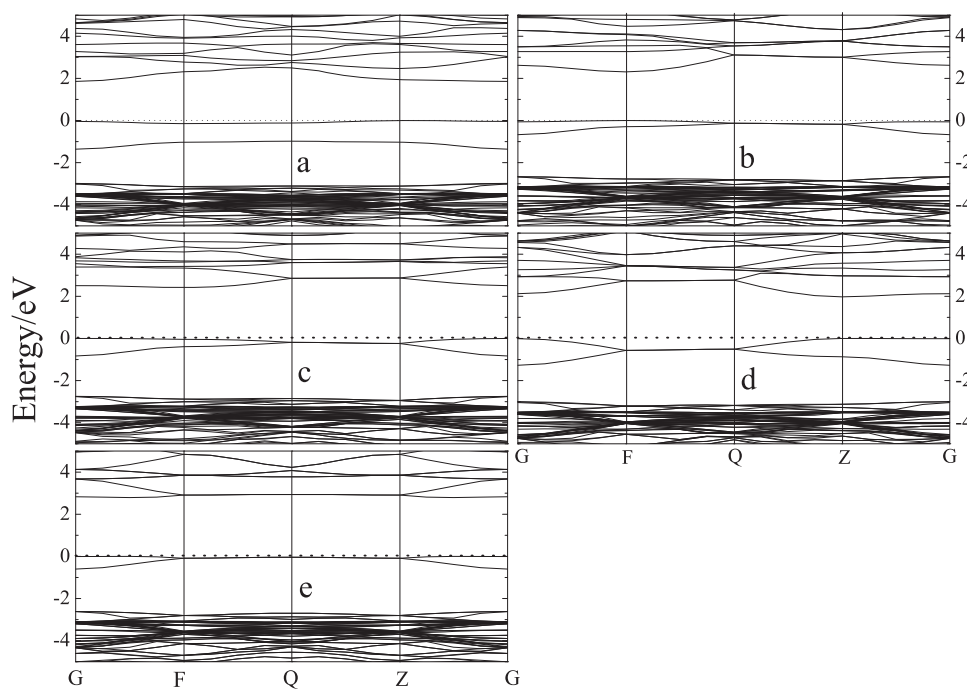


**FIG. 5.** Band structures of MgO supercell with different  $V_O$  pairs. a-e are configurations (1, 2-5), respectively.

Based on the results above mentioned, we have further studied the  $V_O$ -filaments consist of three and four  $V_O$ -chains, respectively. Since the  $V_O$ -filaments tend to be aggregation state, we can build the model for filaments consist of three and four  $V_O$ -chains, as shown in figure 7d and 7e. After geometry optimization and energy calculation, we can get the formation energy per  $V_O$  for two systems, as shown in Table II. The formation energy per  $V_O$ -chain is much smaller than that of one isolated  $V_O$ -chain, which comes from the interaction of  $V_O$ -chains.

Figure 8 and Figure 9 show band structure and corresponding DOS for  $V_O$ -chains above mentioned. It can be seen that one

$V_O$ -chain presents semiconductor properties, with the 1.20 eV energy gap between impurity band and conduction band. For two  $V_O$ -chains in the supercell, there is significant difference in electronic properties between nearest neighbor state and separation state. When two  $V_O$ -chains are in separation state, the gap between impurity band and conduction band is 1.1 eV. The impurity band for this configuration is narrow, which is similar to that for one  $V_O$ -chain. However, when two  $V_O$ -chains are in nearest neighbor state, the impurity band spread more wide than that of separation state. Based the discussion above, we suggest that it comes from the interaction between  $V_O$ -chains. Furthermore, the gap between impurity band and conduction band is 0.67 eV, which is much smaller than that of separation state. Therefore, the aggregation of  $V_O$ -chains can reduce the formation energy and enhance the conductivity of system significantly.

For filament with three  $V_O$ -chains, the impurity bands are dispersed in the most of gap. The gap between impurity bands and conduction bands reduces to zero, which means the conductivity of system is enhanced significantly compared with filament with two  $V_O$ -chains. Nevertheless, the overlap between the top of impurity bands and the bottom of conduction bands is very small. This means few electrons can be accelerated in the conduction bands. Therefore, the system might present semimetal properties under this condition.

**TABLE II.** Formation energy per oxygen vacancy for  $V_O$  filaments with various chains.

configuration	One chain	double chains		Three chains	Four chains
		separation	nearest		
Formation Energy (eV)		1.133	1.140	0.991	0.889
					0.804

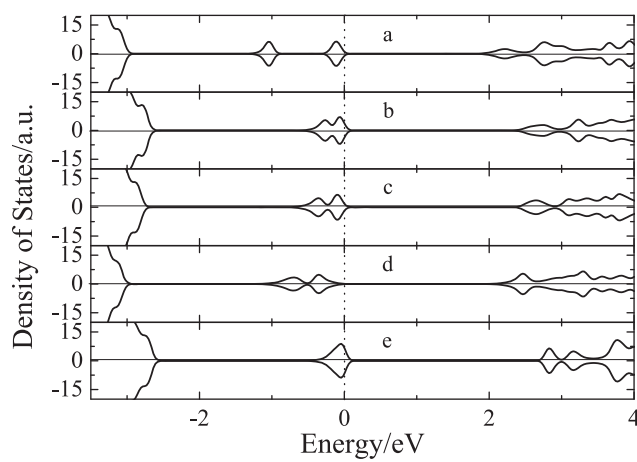


**FIG. 6.** total density of states for MgO supercell with different  $V_O$  pairs. a-e are configurations (1, 2-5), respectively.

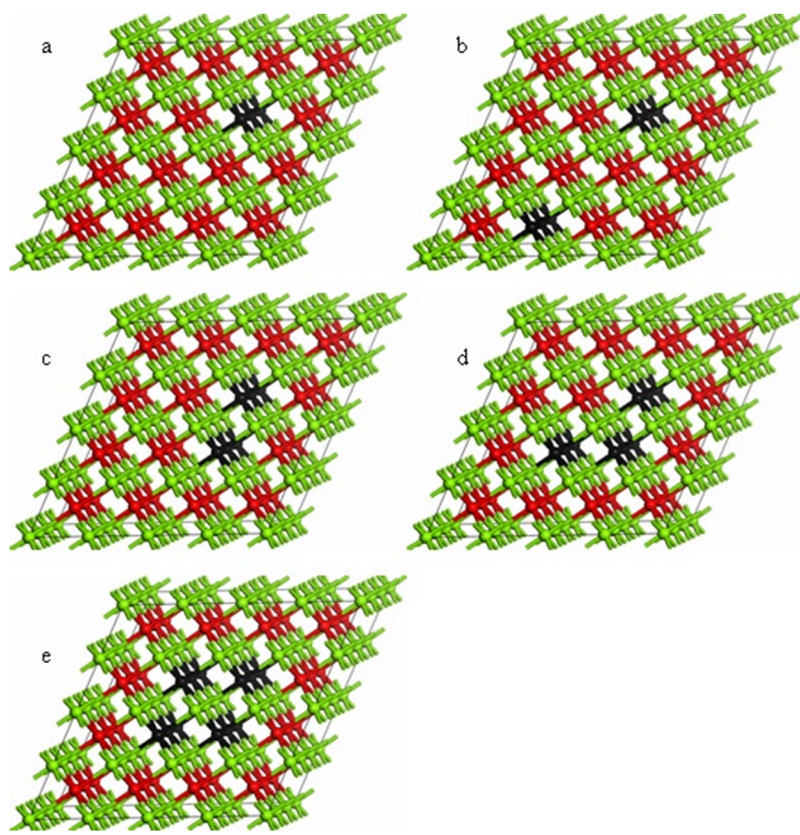


**FIG. 7.** Models of filaments containing various  $V_O$ -chains in  $4 \times 4 \times 3$  MgO supercell. a, a single  $V_O$ -chain. b, double  $V_O$ -chains with separation state. c, double  $V_O$ -chains with nearest neighbor state. d and e are three and four  $V_O$ -chains, respectively.

On the other hand, for filament with four  $V_O$ -chains, the overlap between impurity bands and conduction bands is obviously, and the Fermi level crosses the conduction bands. This means the filaments consisted of four  $V_O$ -chains present metal characters. Based on the

discussion on  $V_O$  impurity band mentioned above, it is reasonable to suggest that the DOS near the Fermi level is mainly consisted of Mg-2p states, and the conductivity is contributed mainly by Mg chains.

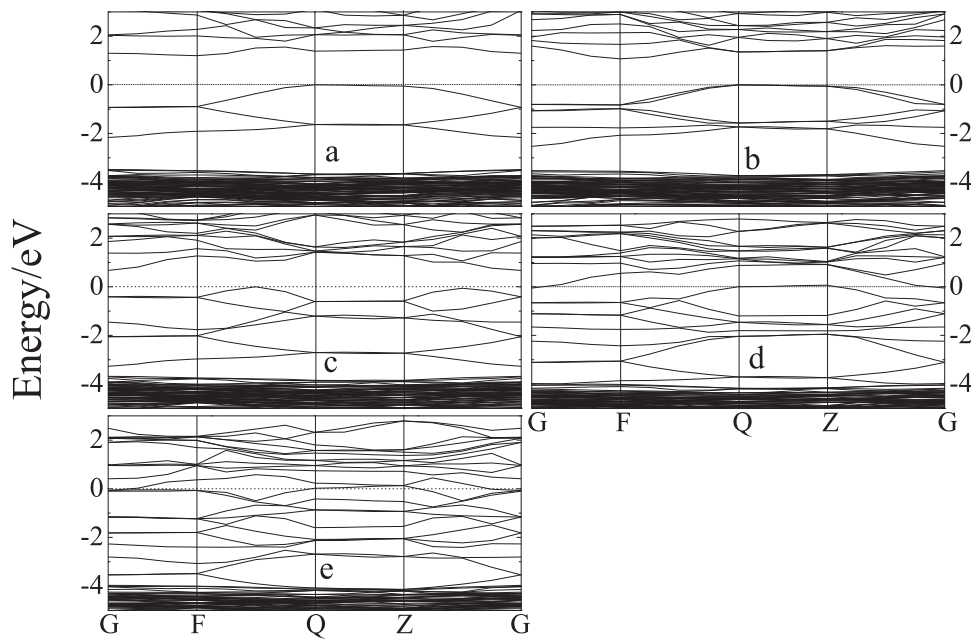


**FIG. 8.** Band structure for filaments containing various  $V_O$ -chains in  $4 \times 4 \times 3$  MgO supercell. a, a single  $V_O$ -chain. b, double  $V_O$ -chains with separation state. c, double  $V_O$ -chains with nearest neighbor state. d and e are three and four  $V_O$ -chains, respectively.

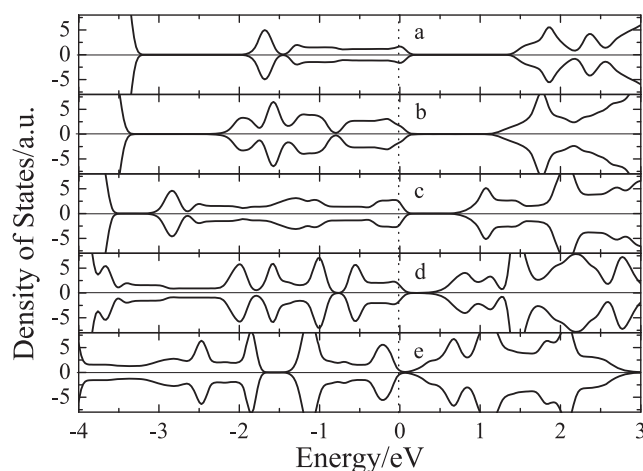


**FIG. 9.** Density of states for filaments containing various  $V_O$ -chains in  $4 \times 4 \times 3$  MgO supercell. a, a single  $V_O$ -chain. b, double  $V_O$ -chains with separation state. c, double  $V_O$ -chains with nearest neighbor state. d and e are three and four  $V_O$ -chains, respectively.

It should be noted that the above results are based on the underestimation of the band-gap as a result of using the PBE functional. To check the tendency of band gap with the raise of clustering vacancies, considering the local effect of O-2p electrons, we performed calculation using PBE+U method for one  $V_O$  doped and vary  $V_O$ -chains models. After calculation test, we take  $U=0.6$  eV for O-2p electrons. With this method, the calculated band gap for purity MgO is 6.23 eV, which is close to the experiment results. The calculated density of states is shown in Figure 10. We can find the defect level sits 3.33 eV below the conduction band for supercell with one  $V_O$  defect, which is close to the results of HSE06 function (3.6 eV). From the figure we can also find the gap between the impurity band and conduction band decrease with the number of chains increase and the gap reduces to 0.20 eV for four chains configuration. The tendency of

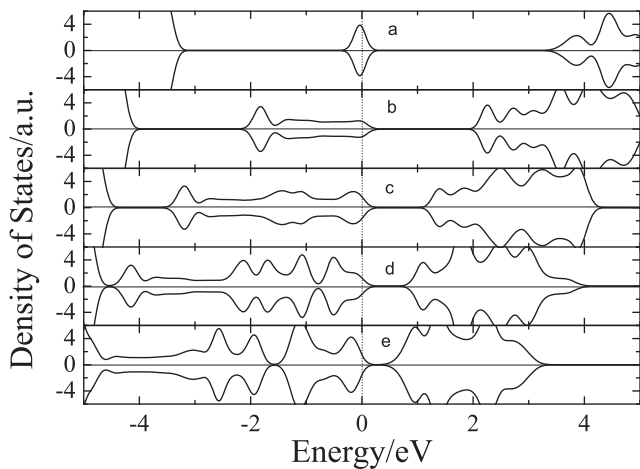


**FIG. 10.** Density of states calculated by PBE+U method for a, MgO supercell with one  $V_O$  defect. b-e, is a single  $V_O$ -chain, double  $V_O$ -chains, three and four  $V_O$ -chains, respectively.

band gap with the raise of clustering vacancies is similar to the results with GGA calculation.

We can descript the set process based our calculation results. During the set process of resistive switching, the new oxygen vacancies tend to form near the initial vacancy, inducing the small clusters. Then the cluster linked each other in chains, creating a conduction filament. The  $V_O$ -filaments growth and connect the bottom and top electrode, resulting in low resistance state. Current compliance plays an important role in this process, which can protect the insulator from hard breakdown and modulate the resistance of LRS. For MgO based resistive switching devices, because of Joule heat of formed  $V_O$ -chains and the aggregation of  $V_O$ -chain, as we discussed above, the large current compliance can induce  $V_O$ -filaments with large diameter, which contains more  $V_O$ -chains. Furthermore, with the increase of diameter of  $V_O$ -filaments, the semiconductor-metal transition occurs. This means the conductivity increase significantly with the increase of  $V_O$ -filament diameter. Therefore, the resistance decreases with the increase of current compliance, not only because of the increase of  $V_O$ -filament diameter, but also because of the increase of conductivity of filaments. Chiu et al report that the resistance of LRS for  $I_{compl}=0.1$  mA is much lower than that for  $I_{compl}=0.5$  mA, which agrees with our conclusion, although more less compliance current are not marked in their literature. In fact, similar phenomenon can be found in many RS devices, which can also be explained by the conclusion above mentioned. It should be noted that, the LRS with semiconductor properties has not been reported till today and simultaneously the RS data for MgO based nonvolatile memory devices with compliance current less than 0.1 mA is lack. These might arise from the unstable of tiny  $V_O$ -filaments because of the activity properties of magnesium nanowires.

In conclusion, the interaction between  $V_O$ s in MgO is studied. The interaction between  $V_O$ s can reduce formation energy of  $V_O$ , resulting in its aggregation. The interaction between  $V_O$ -chains in MgO is also studied. The calculated results show the  $V_O$ -chains tend to growth with nearest neighbor state, which can response to the dependence of diameter of  $V_O$ -filaments on compliance current. With the increase of diameter, the  $V_O$ -filaments present transition of semiconductor-metal. Our calculation reveals the mechanism of growth of  $V_O$ -filaments and according with the existing data in experiments well.

## ACKNOWLEDGMENTS

This work is financially supported by the Foundation of Civil Aviation University of China (Grant no. 31220162012).

## REFERENCES

- S. Seo, M.-J. Lee, D. H. Seo, E. J. Jeoung, D.-S. Suh, Y. S. Joung, I.-K. Yoo, I. R. Hwang, S. H. Kim, I. S. Byun, J.-S. Kim, J. S. Choi, and B. H. Park, "Reproducible resistance switching in polycrystalline NiO films," *Applied Physics Letters* **85**, 5655–5657 (2004).
- R. Waser and M. Aono, "Nanoionics-based resistive switching memories," *Nature Materials* **6**, 833–840 (2007).
- V. K. Sangwan, H.-S. Lee, H. Bergeron, I. Balla, M. E. Beck, K.-Sh. Chen, and M. C. Hersam, "Multi-terminal memristors from polycrystalline monolayer molybdenum disulfide," *Nature* **554**, 500–504 (2018).
- H. Yan and Zh.-Q. Li, "A study on set process and its influence on performance of resistive switching," *Phys. Status Solidi A* **214**, 1700546 (2017).

- <sup>5</sup>S. Roy, S. Maikap, G. Sreekanth, M. Dutta, D. Jana, Y. Y. Chen, and J. R. Yang, "Improved resistive switching phenomena and mechanism using Cu-Al alloy in a new Cu:AlO<sub>x</sub>/TaO<sub>x</sub>/TiN structure," *J. Alloys Compd.* **637**, 517 (2015).
- <sup>6</sup>J. Molina, R. Thamankar, and K. L. Pey, "Performance of ultra-thin HfO<sub>2</sub>-based MIM devices after oxygen modulation and post-metallization annealing in N<sub>2</sub>," *Phys. Status Solidi A* **213**, 1807 (2016).
- <sup>7</sup>L. Goux, K. Opsomer, R. Degraeve, R. Muller, C. Detavernier, D. J. Wouters, M. Jurczak, L. Altimime, and J. A. Kittl, "Influence of the Cu-Te composition and microstructure on the resistive switching of Cu-Te/Al<sub>2</sub>O<sub>3</sub>/Si cells," *Appl. Phys. Lett.* **99**, 053502 (2011).
- <sup>8</sup>M. J. Wang, F. Zeng, S. Gao, C. Song, and F. Pan, "Multi-mode resistive switching behaviors induced by modifying Ti interlayer thickness and operation scheme," *J. Alloys Compd.* **667**, 219 (2016).
- <sup>9</sup>K. Bogle, R. Narwade, A. Phatangare, S. Dahiwale, M. Mahabole, and R. Khairnar, "Optically modulated resistive switching in BiFeO<sub>3</sub> thin film," *Phys. Status Solidi A* **213**, 2183 (2016).
- <sup>10</sup>D. Choi and Ch. S. Kim, "Coexistence of unipolar and bipolar resistive switching in Pt/NiO/Pt," *Applied Physics Letters* **104**, 193507 (2014).
- <sup>11</sup>D. J. J. Loy, P. A. Dananjaya, X. L. Hong, D. P. Shum, and W. S. Lew, "Conduction mechanisms on high retention annealed MgO-based resistive switching memory devices," *Scientific Reports* **8**, 14774 (2018).
- <sup>12</sup>J. Guo, S. Ren, L. Wu, X. Kang, W. Chen, and X. Zhao, "Low-power, high-uniform, and forming-free resistive memory based on Mg-deficient amorphous MgO film with rough surface," *Applied Surface Science* **434**, 1074–1078 (2018).
- <sup>13</sup>F.-C. Chiu, W.-C. Shih, and J.-J. Feng, "Conduction mechanism of resistive switching films in MgO memory devices," *J. Appl. Phys.* **111**, 094104 (2012).
- <sup>14</sup>K.-H. Xue and X.-S. Miao, "Oxygen vacancy chain and conductive filament formation in hafnia," *J. Appl. Phys.* **123**, 161505 (2018).
- <sup>15</sup>S. S. P. Parkin, C. Kaiser, A. Panchula, P. M. Rice, B. Hughes, M. Samant, and S.-H. Yang, "Giant tunnelling magnetoresistance at room temperature with MgO(100) tunnel barriers," *Nat. Mater.* **3**, 862–867 (2004).
- <sup>16</sup>H.-H. Huang, W.-C. Shih, and C.-H. Lai, "Nonpolar resistive switching in the Pt/MgO/Pt nonvolatile memory device," *Applied Physics Letters* **96**, 193505 (2010).
- <sup>17</sup>C. Dias, L. M. Guerra, B. D. Bordalo, H. Lv, M. A. Ferraria, A. M. Botelho do Rego, S. Cardoso, P. P. Freitas, and J. Ventura, "Voltage-polarity dependent multi-mode resistive switching on sputtered MgO nanostructures," *Phys. Chem. Chem. Phys.* **19**, 10898–10904 (2017).
- <sup>18</sup>M. D. Segall, P. J. D. Lindan, M. J. Probert *et al.*, "First-principles simulation: Ideas, illustrations and the CASTEP code," *J. Phys.: Condens. Matter* **14**, 2717–2744 (2002).
- <sup>19</sup>D. Vanderbilt, "Soft self-consistent pseudopotentials in a generalized eigenvalue formalism," *Phys. Rev. B* **41**, 7892–7895 (1990).
- <sup>20</sup>J. P. Perdew, K. Burke, and M. Ernzerhof, "Generalized gradient approximation made simple," *Phys. Rev. Lett.* **77**, 3865–3868 (1996).
- <sup>21</sup>T. H. Fischer and J. Almlöf, "General methods for geometry and wave function optimization," *J. Phys. Chem.* **96**, 9768–9774 (1992).
- <sup>22</sup>B. J. Skinner, "The thermal expansion of thoria, periclase and diamond," *American Mineralogist* **42**, 39–55 (1957).
- <sup>23</sup>T. Yamamoto and T. Mizoguchi, "First principles study on oxygen vacancy formation in rock salt-type oxides MO (M: Mg, Ca, Sr and Ba)," *Ceramics International* **39**, S287–S292 (2013).
- <sup>24</sup>R. C. Whited, C. J. Flaten, and W. C. Walker, "Exciton thermorelectance of MgO and CaO," *Solid State Communications* **13**, 1903 (1973).
- <sup>25</sup>H. J. Monkhorst and J. D. Pack, "Special points for Brillouin-zone integrations," *Phys. Rev. B* **13**, 5188–5192 (1976).
- <sup>26</sup>A. F. Kohan, G. Ceder, D. Morgan, and C. G. Van de Walle, "First-principles study of native point defects in ZnO," *Phys. Rev. B* **61**, 15019 (2000).
- <sup>27</sup>P. Rinke, A. Schleife, E. Kioupakis, A. Janotti, C. Rodl, F. Bechstedt, M. Scheffler, and C. G. Van de Walle, "First-principles optical spectra for F centers in MgO," *Phys. Rev. Lett.* **108**, 126404 (2012).
- <sup>28</sup>S. Prada, L. Giordano, G. Pacchioni, and J. Goniakowski, "Theoretical description of metal/oxide interfacial properties: The case of MgO/Ag(001)," *Applied Surface Science* **390**, 578–582 (2016).
- <sup>29</sup>F. Vines, O. Lamiel-Garcia, K. C. Ko, J. Y. Lee, and F. Illas, "Systematic study of the effect of HSE functional internal parameters on the electronic structure and band gap of a representative set of metal oxides," *Journal of Computational Chemistry* **38**, 781–789 (2017).